Available online at www.sciencedirect.com
ScienceDirect
Journal of the European Ceramic Society 31 (2011) 321–329
www.elsevier.com/locate/jeurceramsoc

A novel low-clay translucent whiteware based on anorthite

Ahmet Capoglu *

Department of Materials Science and Engineering, Gebze Institute of Technology, Istanbul Cad. No: 101, PO Box 141, 41400 Gebze, Kocaeli, Turkey

Received 4 June 2010; received in revised form 26 September 2010; accepted 3 October 2010
Available online 3 November 2010

Abstract

This study was carried out to characterize the properties of a novel low-clay translucent whiteware suitable for daily use. The low-clay whiteware is produced from coarsely and finely milled prefired materials of the same composition plus a small amount of clay. It consists of anorthite ($CaO{\cdot}Al_2O_3{\cdot}2SiO_2$) and mullite ($3Al_2O_3{\cdot}2SiO_2$) crystalline phases and a glassy phase with high crystalline to glassy phase ratio. The development of needle shaped long mullite crystals that were forming three dimensional interlocking network had significant effect on the elimination of pyroplastic deformation during glaze firing. Typical flexural strength and fracture toughness values were ~110 MPa and ~1.85 $MPam^{1/2}$, respectively. The low-clay whiteware had relatively low (4.6×10^{-6}/°C) thermal expansion coefficient which made possible to glaze the whiteware with a typical hard porcelain glaze. A continuous interface layer was produced between the whiteware and the glaze and no crack was present through layer because of expansion mismatch.

Keywords: Anorthite; Low-clay; Pyroplastic; Strength; Translucent; Whiteware

1. Introduction

Whiteware ceramics are defined as highly dense, fired products consisting of glazed or unglazed ceramic bodies that are commonly white, translucent and of fine texture.[1,2] Hard porcelains, bone chinas and fine translucent chinas are the three main types of commercial translucent whitewares which dominate the upper end of the tableware market.

Bone china is made from a mixture of calcined animal bone (50 wt.%), china clay (25 wt.%) and Cornish Stone or feldspar (25 wt.%).[3–5] It is first fired at ~1230 °C while being supported with kiln furniture till to full densification and then the glaze applied and fired on at 1050–1100 °C under the condition of a different heating cycle. Bone china is highly crystalline (~70% crystalline) material with the properties of being resistant to edge chipping and a high flexural strength value of ~100 MPa.[1,4,6] Bone china is also the whitest pottery among the others and prized for its unique appearance. However, it is not very suitable in severe service conditions such as hotels and restaurants because its alkaline rich glaze is easily scratched. Furthermore, it softens during firing and becomes pyroplastic so that it cannot retain its shape unless it is supported by refractory furniture.[7,8]

Hard porcelain is made from a mixture of kaolin (50 wt.%), quartz (25 wt.%) and feldspar (25 wt.%).[2,5,6,9] The shaped objects of hard porcelain are firstly biscuit fired at about 1000 °C, then they are raw glazed and glost fired at around 1400 °C under a reducing atmosphere. Because of its high glassy content (~70%) hard porcelain has low strength (~50 MPa) and is prone to edge chipping, but its silica-rich, hard glaze is both chemically durable and abrasion resistant.[1,2,9–12]

Fine translucent china basically consists of kaolin (30–40 wt.%), feldspar (25–40 wt.%) and quartz (30–50 wt.%).[13] The body has low clay content but more feldspar and quartz which improve the translucency. Fine translucent china is essentially soft porcelain being biscuit fired at about 1230 °C and glost fired at 1150 °C. Fine translucent china is expected to have lower values of strength and fracture toughness than bone china since it contains more glassy phase and it has also easily scratched glaze similar to bone china.[1]

Although, these translucent whitewares have some advantages over each other, so far there has not been any single whiteware whose properties fulfill the tableware market requirements such as high degree of whiteness, translucency, strength (≥100 MPa), edge chipping resistance and having a glaze with

* Tel.: +90 262 6051778; fax: +90 262 6538490.
E-mail address: capoglu@gyte.edu.tr

0955-2219/$ – see front matter © 2010 Elsevier Ltd. All rights reserved.
doi:10.1016/j.jeurceramsoc.2010.10.004

Table 1
Nominal compositions of the prefired materials and their pyroplastic deformation behaviour.

Codes	$CaCO_3$ (wt.%)	$Al(OH)_3$ (wt.%)	SiO_2 (wt.%)	$MgCO_3{\cdot}Mg(OH)_2{\cdot}5H_2O$ (wt.%)	Pyroplastic deformation percentage
A	24.40	38.05	32.85	4.70	27.3
B	20.40	39.30	37.90	2.40	5,5
C	19.35	40.60	37.70	2.35	0,0

high scratch resistance and chemical durability. Therefore, there was a need for the development of a novel whiteware. In the design and development process of this novel whiteware that meets tableware market requirements the following objectives and constraints should be taken into account:

Whiteware should densify at a temperature higher than that used for glazing.

A glaze for the whiteware should have high silica content to be scratch resistant and chemically durable. Although such a glaze will require a high firing temperature (e.g. 1350 °C) and it will have a rather low thermal expansion coefficient (TEC).

Whiteware microstructure should consist of phases with low TECs for well glaze fitting and high thermal shock resistance.

Whiteware should not deform pyroplastically during glaze firing which requires low glassy phase content and the presence of creep inhibiting inclusions.

Whiteware should have a high crystalline to glassy phase ratio and a low residual porosity to maximise the strength and edge chipping resistance (fracture toughness).

In order to achieve a high degree of translucency, fired whiteware should consist of phases whose refractive indices are close to that of the glass phase (∼1.5) and low amount of residual porosities.

By considering above objectives and constraints a concept solution to make a novel whiteware was offered and called as low-clay translucent whiteware.

The low-clay translucent whiteware is based on the use of coarsely and finely milled prefired materials of the same composition, and a low amount of clay.[14,15] The prefired material is composed of ∼65% anorthite ($CaO{\cdot}Al_2O_3{\cdot}2SiO_2$) as the major phase with ∼15% mullite ($3Al_2O_3{\cdot}2SiO_2$) and ∼20% glass as minor phases. The reason for using lower amount of clay (∼10–15%) than the usual (∼30–60%) is to reduce or eliminate the deleterious effects of clay platelet alignment and to keep colouring oxides at a low level for whiteness. Clay particle alignment causes anisotropic shrinkage, which on the macro scale, leads to shape distortion and the formation of differential shrinkage fissures that can act as fracture initiating flaws.[16,17]

The preparation and the characterization of the prefired materials were carried out in detail in a previous study.[18] In this study, the idea of the concept solution was implemented to design and prepare the final whiteware body using these prefired materials and low amount of clay as raw materials. However, further characterization of prefired materials was carried out to optimize the composition affecting the pyroplastic deformation behaviour prior to preparation of final body. After the sintering and glazing studies the resultant whiteware was characterized using strength and toughness measurements, colour measurement, dilatometer technique, X-ray diffraction (XRD), and scanning electron microscopy (SEM).

2. Experimental

From the previous study,[18] it was observed that there was a strong relationship between the elimination of pyroplastic deformation and the development of mullite crystals in the microstructure of prefired materials. Before the preparation of final body using prefired materials detailed pyroplastic deformation study was conducted on the selected three prefired compositions (Table 1) to understand this relationship deeply. The details of raw materials and the preparation method of prefired materials are explained in details elsewhere.[18] For the assessment of pyroplastic deformation behaviour, rectangular bars with the dimensions of 20 mm × 120 mm × ∼4 mm were produced using moist granules of prefired materials. The bars were double fired to replicate both biscuit and glaze firings. For biscuit firing, specimens were fired at 1370 °C for 3 h on a wholly supporting tile and following that the specimens were re-fired at 1350 °C for 1 h on the brick while being supported only at their ends for glaze firing. On the completion of firings, the amount of pyroplastic deformation of a bar was measured by determining the value of d, which is a measure of how the bar has sagged as shown in Fig. 1. The pyroplastic deformation percentage was then calculated as; $(d/D) \times 100$, where D is the unsupported length of the bar, i.e. 85 mm. To determine d, a metal bar, 85 mm long, was placed against the sagged ceramic bar on the concave side so that its ends were equidistant from those of the ceramic bar and d measured using a vernier caliper.

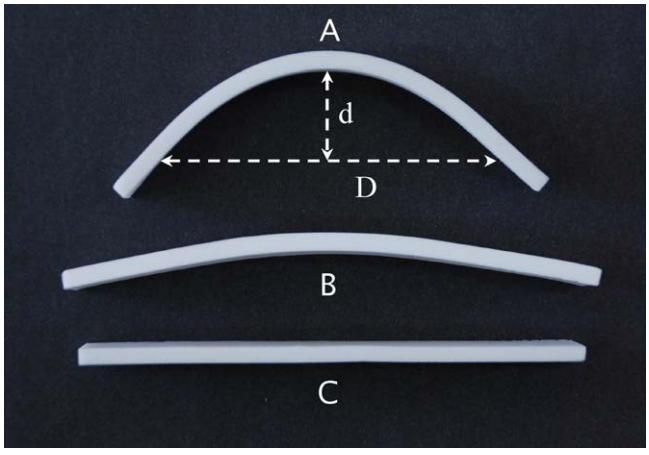

Fig. 1. Pyropastically deformed and un-deformed test bars of prefired materials with different compositions.

Table 2
Chemical compositions of Ukrainian ball clay and a commercial hard porcelain glaze used in the study.

Constituents (wt.%)	Ukrainian ball clay	Hard porcelain glaze
SiO_2	59.62	66.87
Al_2O_3	27.41	13.78
CaO	0.28	7.05
MgO	0.51	1.45
Na_2O	0.49	0.95
K_2O	1.93	1.88
TiO_2	1.37	0.12
Fe_2O_3	0.82	0.16
SO_4	0.08	0.11
L.O.I.	7.49	7.63

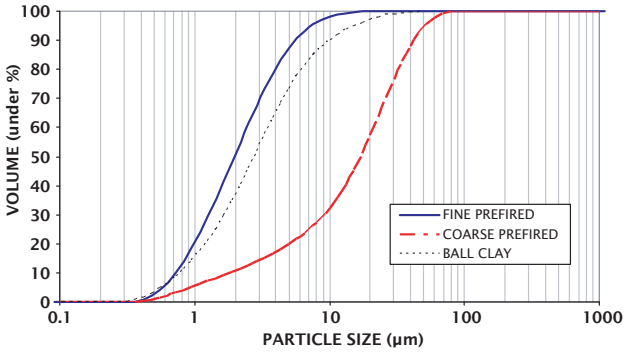

Fig. 2. Particle size distributions of coarse, fine prefired materials and ball clay.

To correlate the pyroplastic deformation with the crystalline phases developed in the microstructure, the sintered samples were analysed by XRD and SEM techniques. Powdered form of sintered samples of prefired bodies were scanned from $2\theta = 10$–70°, at a scanning speed of 1°/min, using a RIGAKU 2000 DMAX diffractometer (with $Cu_{K\alpha}$-radiation, $\lambda = 0.154$ nm) at 40 kV and 40 mA for XRD analysis. The specimens were prepared for SEM observations by polishing with 6, 3, 1 μm diamond pastes after grinding with silicon carbide papers as abrasive and lubricated with water. The polished surfaces of specimens were chemically etched in 5% HF solution for 60 s. A Phillips XL30 SFEG scanning electron microscope (operating at 15 kV) was used for microstructural examination of samples with secondary electron images (SEI) used predominantly.

The final body of low-clay whiteware was formulated as 50% coarse prefired material (~20 μm), 38% fine prefired material (~2.0 μm) with the same composition (denoted as C in Table 1) and 12% clay. The clay used for the whiteware body preparation was a Ukrainian ball clay type and was obtained from Kale Minerals Co., Turkey. The ball clay had the composition or impurity contents shown in Table 2. The mineralogical analysis indicated that the Ukrainian ball clay was mainly in kaolinite form (38 wt.%), some other crystalline constituents which were quartz (20 wt.%), illite (16 wt.%) and the mixture of tabular clayey minerals (16 wt.%) present. Also, montmorillonite (4 wt.%), amorphous phase (3 wt.%) and anatase (3 wt.%) were present as minor compounds in the Ukrainian ball clay. The XRF chemical analysis result of the final body of low-clay whiteware is given in Table 3. The particle size distributions of powders were analysed by a Malvern Mastersizer μ + Ver.2.15 model laser diffraction particle size analyser. Typical particle size distributions of coarse and fine prefired materials and clay are given in Fig. 2. To obtain a homogeneous mixture, prefired materials and clays were wet mixed/milled for 1 h in a porcelain pot containing alumina balls. After mixing/milling, some slurry was withdrawn for particle size analysis and the remaining slurry was transferred to the plastic container and oven dried at ~110 °C. The product of drying process was a powder cake which was broken up to form a powder, which was then granulated by first spraying with a fine mist of water droplets and then by agitating the damp powder.

The fusibility and firing behaviour of the final body of low-clay whiteware was investigated by the employment of a heating microscope (MISURA, Expert System Solutions, Italy). The rectangular shaped sample of the final whiteware body was heated up to 1400 °C at a constant heating rate of 10 °C/min and the changes on the shape of samples during heating was optically monitored and recorded by a dedicated computer.

The change in densification and mechanical behaviour of the final body of low-clay whiteware was investigated by measuring the relevant properties of the actual sintered specimens. While cylindrical pellets having 31.5 mm initial diameter and ~4 mm thickness were prepared for the assessment of sintering study the rectangular bars were prepared for the assessment of mechanical behaviour. To produce cylindrical pellets and rectangular bars the moist granules of the whiteware body were placed in a stainless steel die and uniaxially pressed by means of a hand-operated hydraulic press at 30 MPa being maintained for 60 s. The unfired bars had dimensions of 7 mm × 75 mm × ~4 mm. Both cylindrical pellets and rectangular bars were fired at temperatures from 1290 °C to 1390 °C in a chamber furnace, heated with $MoSi_2$ elements (Nabertherm). The furnace was heated to the peak temperature with soaking times of 3 h at the rate of 3 °C/min and on completion of the soaking period, power to the furnace was automatically shut off and cooling rate was then dictated by the cooling rate of the furnace. The specimens generally remained overnight in the furnace before they were removed. The degree of densification was monitored with the change in relative density which is the ratio between the calculated bulk density and powder density of the sintered specimen. The bulk densities were determined from the volume of pellets and their masses. Powder

Table 3
Typical XRF analysis of the final body of low-clay whiteware.

Oxide	SiO_2	Al_2O_3	CaO	MgO	Na_2O	K_2O	TiO_2	Fe_2O_3
wt.%	42.93	43.62	11.89	0.98	0.03	0.15	0.16	0.19

densities of sintered specimens were measured by He pycnometer (Ultrapycnometer 1000, Quantachrome Instruments).

In order to study the mechanical behaviour of whiteware elastic modulus, flexural strength and fracture toughness were measured. The elastic modulus of sintered specimens was measured at room temperature by the resonance frequency method according to ASTM standard C1259-94 using a Grindo-Sonic system (Grindo-Sonic MkV, J. W. Lemmens, Belgium). The flexural strength of sintered test bars were measured using an electronic universal tester (Model 5569, Instron Ltd.) by a three point bending fixture with a lower span of 50 mm and crosshead speed of 1 mm/min, based on ASTM standard C1161-90. The surface condition of tested specimens was as-sintered. At least eight specimens were used for each sintering temperature. The fracture toughness measurements were realized by microindentation method[19] for which Vickers microhardness values were determined on the polished surface of the fired samples using a microhardness tester with a Vickers indenter (Instron Wolpert® Testor 2100®). The indentations were formed by the application of 9.8 N load for 13 s. The test has been repeated ten times for each specimen. The cracks were measured using the microscope attachment on the microhardness tester (Instron Wolpert® Testor 2100®) immediately after each indentation. Crack measurements were only made on indents that were well defined without chipping and for which the cracks did not terminate at pores.

Thermal expansion behaviour of the final body of low-clay whiteware was measured between room temperature and 700 °C using a NETZSCH dilatometer at a heating rate of 10 °C/min.

The whiteness and colours of the final body of low-clay whiteware, and samples of commercial bone china and hard porcelain were defined using the Minolta CR-300 colorimeter which operates on the CIELab method and in reflection mode. The whiteness and colour of specimens were determined by measuring the three parameters (Hunter parameters) L^* (brightness) from absolute white $L = 100$ to absolute black $L = 0$, a^* (red-green), b^* (yellow blue) elaborated from the visible spectra.

A commercial hard porcelain glaze was obtained from a local hard porcelain manufacturer for the glazing study. The XRF chemical analysis of the commercial glaze used in this study is given in Table 2. One side of the disc shaped biscuit fired specimens was dipped into a glaze slip for the glaze deposition. Then glaze deposited specimens were dried at 110 °C in an oven for 12 h. After drying, the specimens were heat treated for 1 h at 1350 °C for glaze maturing. The glazed specimens were then cut cross sectionally in half and standard procedure for polishing and chemical etching with 5% HF solution was carried out before SEM examination. Microanalysis was also performed using the embedded EDS digital controller and control software.

3. Results and discussion

The prefired material had been primarily designed to obtain a microstructure consisting of anorthite ($CaO{\cdot}Al_2O_3{\cdot}2SiO_2$) crystals as the major phase and glass as a minor phase. Because, anorthite has the required low value of thermal expansion coefficient[20] $\sim 4.3 \times 10^{-6}/°C$ and also has a refractive index[20]

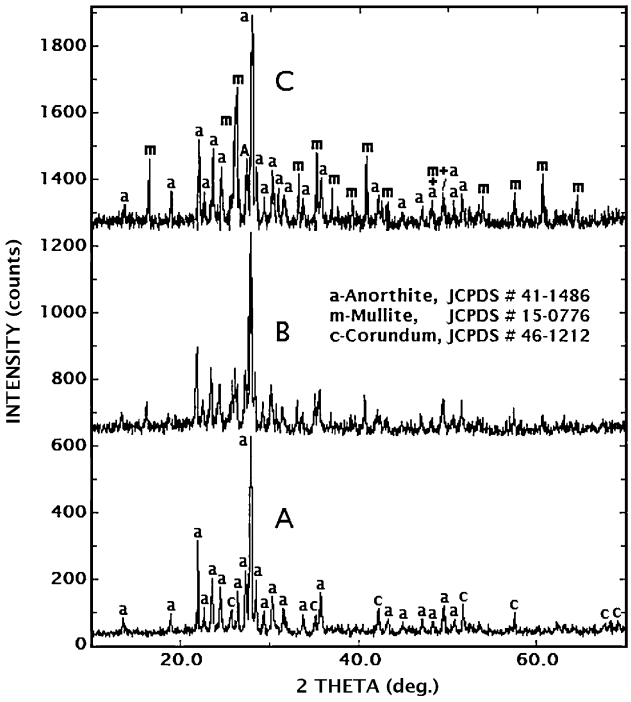

Fig. 3. XRD patterns obtained from pyropastically deformed and un-deformed test bars of prefired materials with different compositions sintered at 1370 °C.

of 1.58 which is close to that of the glass phases (~1.5) in which it is embedded. This is required for enhancing translucency. However, it was understood from the previous study[18] that the anorthite crystals which developed in the microstructure of prefired material were only a few micron in length and were resistant to grow more. These small anorthite crystals were not capable enough to resist the pyroplastic deformation during firings. Therefore, the basic prefired composition was modified to develop an additional crystalline phase which should have creep inhibiting behaviour. Fig. 1 shows the state of the actual tests specimens on which pyroplastic deformation study was carried out after firings. Table 1 lists the calculated pyroplastic deformation percentages of samples shown in Fig. 1. It can be seen from Fig. 1 that as the composition of the prefired material (Table 1) changed the level of pyroplastic deformation was dramatically reduced and finally eliminated completely. The X-ray diffraction patterns and SEM images obtained from the pyroplastically deformed and non-deformed samples are shown in Figs. 3 and 4, respectively. It is apparent that the development of needle shaped mullite ($3Al_2O_3{\cdot}2SiO_2$) crystals and its size and distribution in the microstructure has an important effect on the elimination of pyroplastic deformation. As it can be seen, highly deformed specimen (indicated as A in Figs. 1, 3 and 4) did not develop any mullite but only anorthite crystals in the microstructure while the specimen with a slight deformation (indicated as B in Figs. 1, 3 and 4) developed small amount of needle shaped mullite crystals on top of anorthite. The mullite crystals were piling up locally rather than evenly distributed in the microstructure. However, the specimen that did not show any significant pyroplastic deformation (indicated as C in Figs. 1, 3 and 4) developed more mullite crystals. They were also needle shaped but,

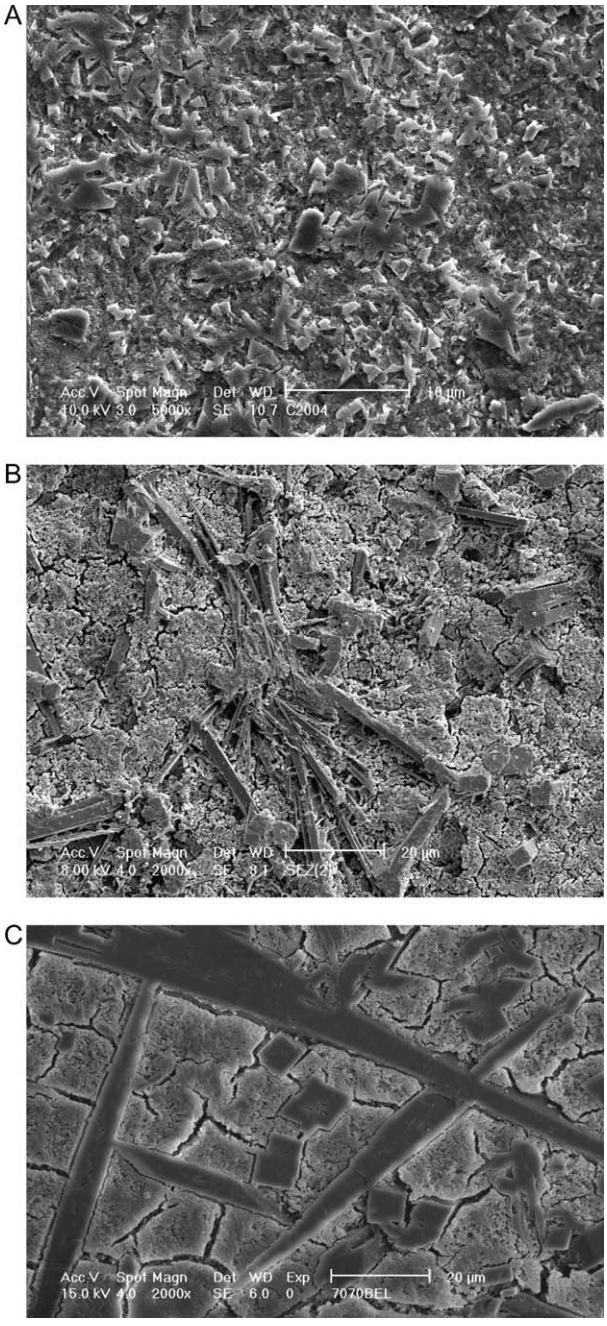

Fig. 4. SEM micrographs of pyropastically deformed and un-deformed test bars of prefired materials with different compositions sintered at 1370 °C.

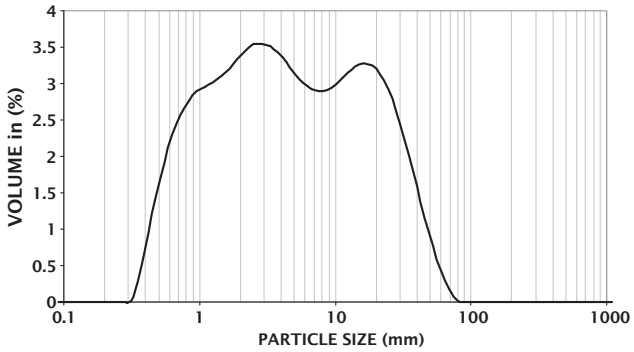

Fig. 5. The particle size distribution of the mixed final body of low-clay whiteware.

longer and thicker than the former one. These needle shaped long mullite crystals which were randomly orientated in the microstructure would form a three dimensional skeleton which would stop the whiteware deforming during glaze firing.

Hence, the final body of low-clay whiteware was prepared with the modified prefired materials having the composition of C in Table 1 fired at 1370 °C for 3 h. The final body consisting of 50 wt.% coarse, 38 wt.% fine prefired materials and 12 wt.% clay was processed and characterized. Typical particle size distribution of the final body is given in Fig. 5. The analysis shows a bimodal distribution presenting two maximum points, which are centered, at around 2 and 20 μm and would allow grouping the particles as coarse and fine and their arrangement in the pressed body would enhance particle packing. As the ratio between coarse and fine particle size is approximately 10, which is large enough for fine particles to fill the gaps between coarse particles.

Conventional hard porcelains are typically fired in the temperature range from 1350 to 1370 °C to both densify and glaze the body. Since the low-clay whiteware is to be coated with a typical hard porcelain glaze it should be fired at the same level of temperature. Therefore, its densification behaviour was studied extensively. The top firing temperature, at which the final body of low-clay whiteware would achieve a high degree of densification via partial vitrification, was determined from the degree of sintering versus temperature graph obtained using a heating microscope. The sintering speed that reaches its maximum is identified in correspondence of the negative peak of the first derivative curve. The steady sintering of the final whiteware body continued up to 1200 °C, beyond which a slow increase in the degree of sintering due to the formation of liquid phase is observed, as the sintering curve is starting to deviate from the base line. A remarkable increase in degree of sintering, by the viscous flow of glassy phase, is observed at above 1300 °C and the maximum sintering is achieved when the temperature reached at around 1370 °C.

The densification behaviour of the final body of low-clay whiteware was also monitored by sintering the specimens from 1290 to 1390 °C with 10 °C intervals to verify the results obtained from heating microscope study. The whiteware body densified well, reached a maximum value of ∼87% relative density at 1350 °C, although the material was not significantly over fired to some 30 °C higher producing quite a large firing range. However, upon further increase in sintering temperature density started to decrease because of bloating i.e., pore volume expansion. Both heating microscope data and sintering study results are in accord with the obtainment of maximum densification temperature.

The phases developed in the final body of low-clay whiteware during sintering were studied using XRD and SEM techniques. Fig. 6 shows the X-ray diffraction pattern of the final body sintered at 1370 °C. The clay addition to prefired material mixture, for the final body preparation, did not affect the type of crystalline phases developed in the microstructure. The crys-

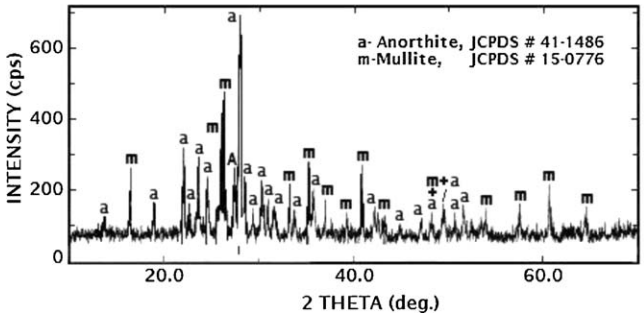

Fig. 6. An XRD pattern obtained from the final body of low-clay translucent whiteware sintered at 1350 °C.

talline phases identified in the specimen are anorthite being the major crystalline phase and mullite as minor crystalline phase labeled as (a) and (m), respectively. Some glassy phases are also present. The SEM micrographs given in Fig. 7(A) and (B) show tabular shaped anorthite crystals (1–3 μm) and needle-shaped mullite crystals (5–10 μm), respectively. The EDS analysis in Fig. 7(C) and (D) confirms the formation of anorthite (marked as a) and mullite crystals (marked as m). The glassy phase (marked as g) which is etched away to reveal the crystalline phases, are distributed between the crystals. It was observed that those long mullite crystals (20–80 μm) which were formed in the prefired materials and broken up during milling the prefired materials prior forming the final body of low-clay whiteware did not grow significantly further during sintering the final body.

Fig. 8 shows the elastic modulus and flexural strength behaviour of the final body of low-clay whiteware sintered in the temperature range from 1290 to 1390 °C. Both elastic

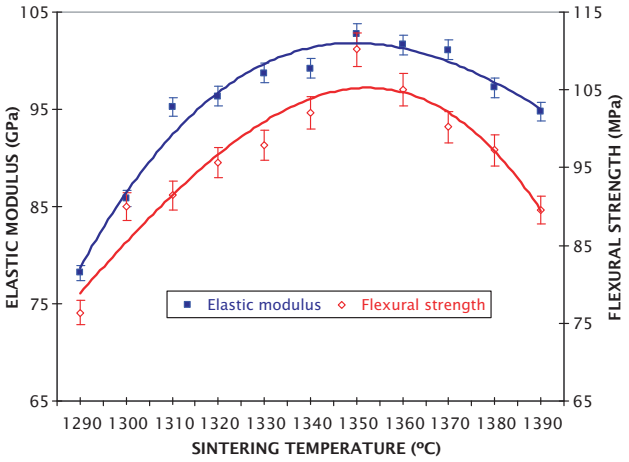

Fig. 8. Variation in elastic modulus and flexural strength values of the low-clay whiteware with sintering temperature.

modulus and flexural strength of the sintered material varied proportionally to its relative density. The elastic modulus which is an index of rigidity of material, increased with sintering temperature following the densification behaviour of low-clay whiteware. Since it provides information about the compactness of microstructure[21] its maximum value could be accepted as the representative of its highest densification degree. The maximum elastic modulus (~102 GPa) of low-clay whiteware was obtained from a sample fired at 1350 °C where also maximum relative density value was reached. The flexural strength of the low-clay whiteware increased with an increase in sintering temperature up to 1350 °C where it attained its maximum. Upon further heating, the flexural strength then decreased with a corresponding decrease in density. The maximum flexural strength

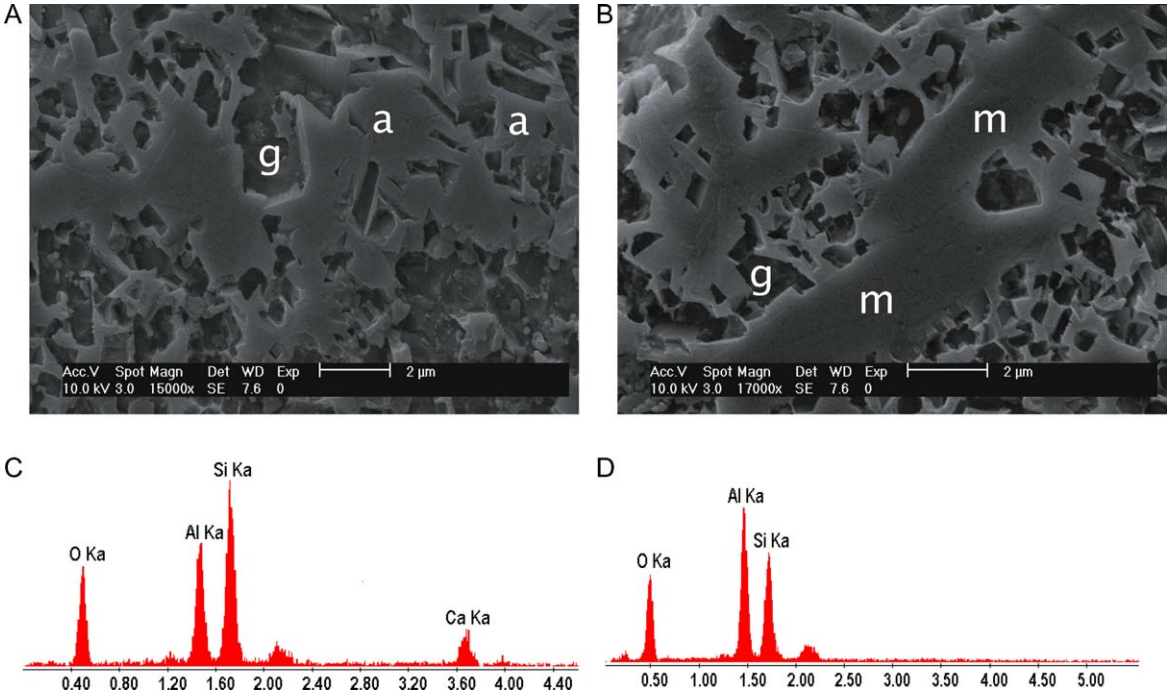

Fig. 7. SEM micrographs of an etched low-clay translucent whiteware sintered at 1350 °C showing (A) anorthite, (B) mullite, and glass formation labelled as a, m, and g, respectively. EDS spectra obtained from (C) anorthite and (D) mullite crystals.

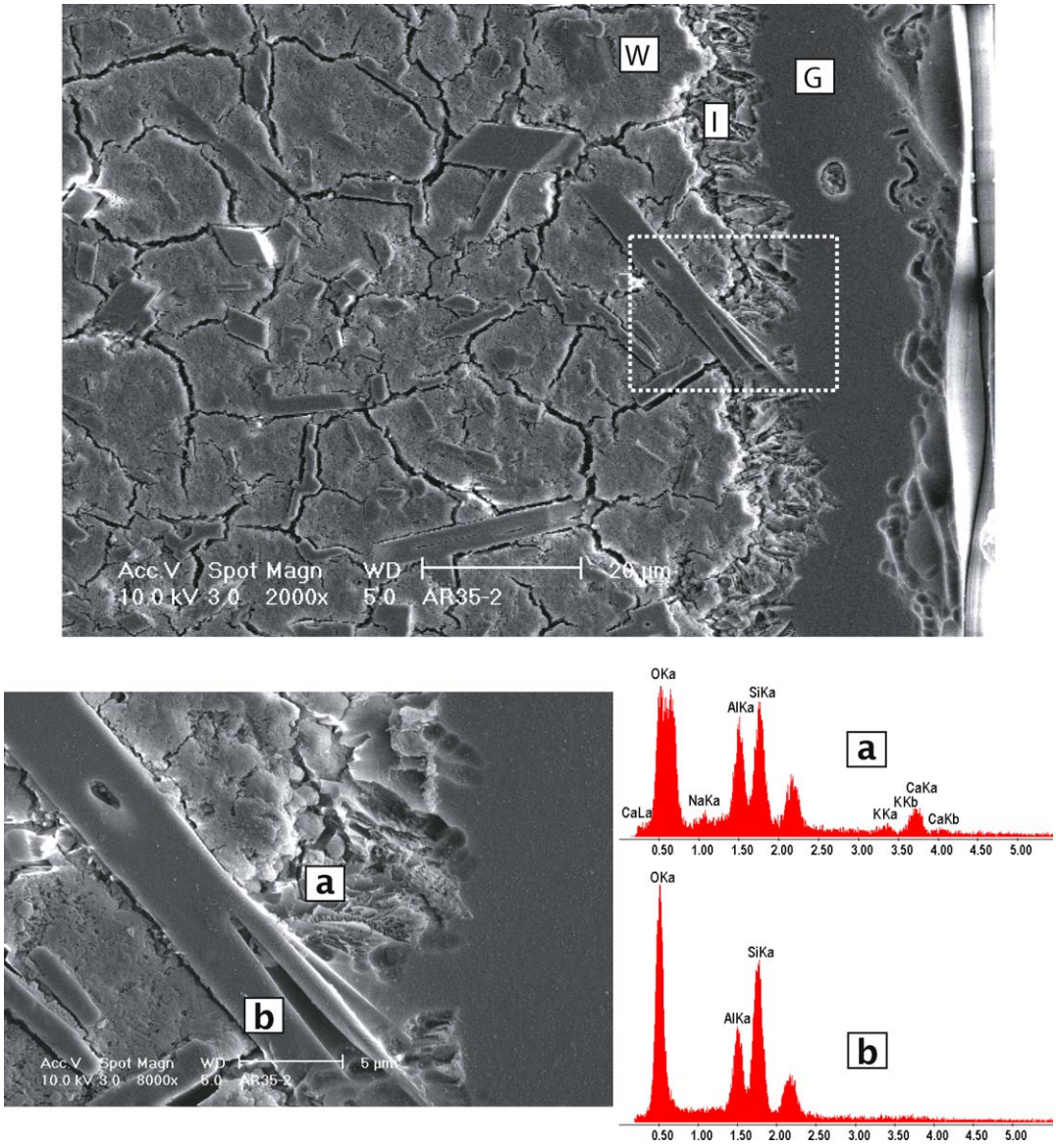

Fig. 9. SEM micrograph of a polished and etched cross section of hard porcelain glaze on the low-clay translucent whiteware showing an interfacial zone (I) between the whiteware (W) and the bulk of the glaze layer (G), (a) and (b) energy dispersive spectra from different regions of interfacial zone.

which also confirmed the maximum relative density obtained from the low-clay whiteware fired at 1350 °C is about 110 MPa is same as to that of bone china but much higher than hard porcelain. The high strength value of bone china compared to hard porcelain was attributed to its high crystalline content. SEM micrographs indicated that the low-clay whiteware also has highly crystalline structure. The fracture toughness of the new whiteware was also measured[22] and typical fracture toughness value obtained from a sample sintered at 1350 °C is 1.85 MPam$^{1/2}$. Fracture toughness showed some variations with sintering temperature. X-ray analysis showed that there were no measurable differences in the degree of crystallinity in these samples; therefore the increase in toughness cannot be attributed to increasing crystallinity or changing ratios of anorthite and mullite crystalline phases. On the other hand, there are considerable differences in the densities of the samples sintered at different temperatures.

The thermal expansion behaviour of the specimen fired at 1350 °C for 3 h was measured between room temperature and 750 °C and the average thermal expansion coefficient (TEC) of the low-clay whiteware over the 25–600 °C temperature range is estimated to be $\sim 4.6 \times 10^{-6}$/°C which is much lower than the TEC value of bone china but similar to hard porcelain and allows the low-clay whiteware to be glazed with certain silica-rich glazes, such as a hard porcelain glaze. This relatively low TEC also indicates that this whiteware would be very resistant to being thermally shocked.

When glazing a ceramic substrate, it is important to avoid the generation of destructive stresses at the glaze/ceramic interface.[23] Stress in the glaze layer develops as a result of difference in thermal contraction between the glaze and the ceramic as they cool from the firing temperature down to room temperature. To prevent excessive and destructive stresses being generated, the thermal expansion coefficient of a glaze should, ideally, be

carefully matched with that of the ceramic, so that it should be same or slightly lower. Commercially available hard porcelain glaze was chosen for glazing the final body of low-clay whiteware. The TEC of the hard porcelain glaze was reported to be[24] $\sim 4.5 \times 10^{-6}/^{\circ}C$ which is very close to the TEC value of the low-clay whiteware ($\sim 4.6 \times 10^{-6}/^{\circ}C$). A cross-section examination of the microstructure developed between a glazing layer of hard porcelain glaze and the low-clay whiteware, heat treated at 1350 °C for 1 h, was carried out using a scanning electron microscopy (Fig. 9). SEM examination of the polished and etched cross-section even at lower magnification reveals clear evidence of an interaction layer formation on samples fired at 1350 °C for 1 h. The crystalline phases at the interface can be clearly distinguished at higher magnification. Fig. 9 shows a typical secondary electron image of such an interfacial zone (I) between the low-clay whiteware (W) and the bulk of the glaze layer (G). The interfacial zone is about 10 μm thick and continuous throughout the interface and this zone appears to be more highly crystalline than the bulk of the glaze layer. However, its crystallization nature differs from the underlying low-clay whiteware. The crystals at the interfacial zone are much smaller than the neighbouring crystals in whiteware section. They are mostly in the form of aggregates of grains less than a micron in diameter embedded in the glaze layer at the interface. Also some needle shaped crystals which had been previously formed in the whiteware microstructure seem to be continued growing into the glaze contributing for the formation of interfacial zone. Energy dispersive spectra from the two different regions at the interfacial zone are given in Fig. 9. The spectrum from region (a) reveals the presence of Ca, Al, Si and some O suggesting most probably that the crystals in the region (a) are anorthite ($CaO{\cdot}Al_2O_3{\cdot}2SiO_2$) and the spectrum from region (b) reveals the presence of Al, Si and some O suggesting most probably that the crystal in the region (b) is mullite ($3Al_2O_3{\cdot}2SiO_2$). Similar observations on the formation of interfacial zone between bone china and advanced borosilicate (ABS) type glaze show that the glassy phase present in the whiteware body plays a significant role in the formation of the interaction layers by helping the creation of a low viscosity melt together with the glaze at higher temperatures, therefore increasing the mobility of the diffusing species.[25] From the point of view of thermal expansion mismatch, the presence of the interfacial zone would be beneficial if its coefficient of thermal expansion was to be intermediate between that of the whiteware and bulk of the glaze. This would be so, because both anorthite and mullite crystals have comparable TEC values to the low-clay whiteware and hard porcelain glaze. Therefore, no crack has been detected in the glaze and/or interaction layer.

The whiteness of whiteware ceramic is crucial for its marketing. To have some idea about the degree of whiteness and to compare this value with the whiteness of commercially available whitewares the whiteness of the low-clay translucent whiteware and two samples of commercial whitewares, namely bone china and hard porcelain were measured. The colour difference values (a^*, b^*) and the L^* parameters (whiteness) are listed in Table 4. It can be seen from Table 4 that negative values of a^* and positive values of b^* were measured from all the samples, indicating that the values lie in the upper left quadrant (green and yellow region) with coordinates. It also appears evident that the variation of a^* and b^* Hunter parameters between low-clay whiteware and the commercial bone china sample is not significant. When the whiteness of the commercial bone china (L^*; ~93) is taken into consideration the obtained value from the low-clay whiteware (L^*; ~94) is quite comparable. This low-clay translucent whiteware owes its high degree of whiteness to its low clay content and the usage of prefired materials which were formed by exploiting raw materials containing low colouring impurities.

Table 4
The degree of whiteness (Hunter parameters) of the final body of low-clay translucent whiteware, and samples of commercially produced bone china and hard porcelain.

Type of whiteware	L	a^*	b^*
Bone china	93.15	−0.43	3.17
Hard porcelain	86.71	−1.12	2.40
Low-clay whiteware	94.04	−0.35	3.03

Even tough it has not been measured quantitatively the translucency of the low-clay whiteware was also quite comparable with commercial bone china sample when it is compared under the transmitted light. The relatively low refractive index value which would facilitate the attainment of translucency has been satisfied with anorthite crystals having a value of 1.58 which is expected to be close to that of the glass phases (~1.5) in which it is embedded. However, on the other hand, mullite has a slightly higher refractive index[5,20] of 1.64 but its low concentration and relatively coarse size of its grains lessens its affect on translucency.

The cost of the low-clay whiteware body could be higher than the presently used hard porcelain and bone china bodies due to the need for the prefired materials. However, if a supplier could provide the prefired materials to the whiteware manufacturers with low-cost then the final product could compete with the present products in the market.

4. Conclusion

A low-clay translucent whiteware which is suitable for high-class hotel and restaurant use; i.e., to be aesthetically pleasing and to be suitable for severe service conditions and combines the best features of bone china, fine translucent china and hard porcelain was designed and fabricated using a mixture of mostly non-plastic prefired materials and Ukranian ball clay and its properties were investigated. The prefired material consisted of anorthite ($CaO{\cdot}Al_2O_3{\cdot}2SiO_2$) as the major phase with mullite ($3Al_2O_3{\cdot}2SiO_2$) and glass as minor phases. It was found that the development of needle shaped long, secondary type mullite crystals which were randomly orientated in the microstructure in the prefired materials, has an important role for eliminating the pyroplastic deformation during glaze firing.

It has been shown that it was possible to densify the low-clay translucent whiteware in the 1350–1380 °C temperature ranges. After sintering, the low-clay whiteware has high crystalline to glassy phase ratio which is beneficial to maximise

strength and fracture toughness. Typical flexural strength and fracture toughness values were ∼110 MPa and ∼1.85 MPam$^{1/2}$, respectively.

Relatively low thermal expansion coefficient ($\sim 4.6 \times 10^{-6}/^{\circ}C$) of low-clay translucent whiteware made possible to glaze the material with a typical high resistant hard porcelain glaze. It was observed that the interface layer produced between the low-clay whiteware and the glaze was continuous and no crack was present through the layer because of thermal expansion mismatch. The low-clay whiteware also possess ultra whiteness and high degree of translucency.

This low-clay whiteware could be manufactured without modifying substantially the process and technological conditions of the present industry.

References

1. Wood RK. Ceramic whiteware. In: Schneider SJ, Davis JR, Davidson GM, Lampman SR, Woods MS, Zorc TB, editors. *Ceramics and glasses, engineered materials handbook*. USA: ASM International; 1991. p. 930–6.
2. Carty WM, Senapati U. Porcelain-raw materials, processing, phase evolution, and mechanical behaviour. *J Am Ceram Soc* 1998;**81**:3–20.
3. Franklin CEL, Forrester AJ. The development of bone china parts I and II. *Trans J Br Ceram Soc* 1975;**74**:141–5.
4. Rado P. *Bone china, ceramics monographs, a handbook of ceramics*. Freiburg i. Brg: Verlag Schmid GmbH; 1981.
5. Dinsdale A. *Pottery science materials, process and products*. West Sussex UK: Ellis Horwood Ltd; 1986.
6. Batista SAF, Messer PF, Hand RJ. Fracture toughness of bone china and hard porcelain. *Br Ceram Trans* 2001;**10**:256–9.
7. Kingery WD, Bowen HK, Uhlmann DR. *Introduction to ceramics*. New York: John Wiley and Sons; 1976.
8. Airey AC, Birtles JF. Pyroplastic deformation of whiteware bodies. In: Henkes VE, Onoda GY, Carty WM, editors. *Science of whitewares*. Westerville, OH: Am Ceram Soc; 1996. p. 225–35.
9. Rado P. *An introduction to the technology of pottery*. Oxford: Pergamon; 1988.
10. Bragança SR, Bergmann CP. A view of whitewares mechanical strength and microstructure. *Ceram Int* 2003;**29**:801–6.
11. Ece OI, Nakagawa Z. Bending strength of porcelains. *Ceram Int* 2002;**28**:131–40.
12. Kobayashi Y, Ohira O, Ohashi Y, Kato E. Effect of firing temperature on bending strength of porcelains for tableware. *J Am Ceram Soc* 1992;**75**:1801–6.
13. Ryan W, Radford C. *Whitewares: production, testing and quality control*. Oxford: Pergamon; 1987.
14. Messer PF, Capoglu A, Jafari M, Mohd Noor AF, Okojie HE. Whiteware ceramic compositions. US Patent; 1998; 5716894.
15. Messer PF, Capoglu A, Jafari M, Mohd Noor AF, Okojie HE. Milled fired material usable in whiteware ceramics. Europe Patent; 1997; EP0787699.
16. Agbarakwe UB, Banda JS, Messer PF. Non-uniformities and pore formation. *Mater Sci Eng A: Struct* 1989;**109**:9–16.
17. Cubbon RCP, Roberts W, Camm J, Walters WL. Clay particle orientation effects in whiteware bodies. *Ceram Eng Sci Proc* 1986;**7**:1213–23.
18. Capoglu A, Messer PF. Design and development of a chamotte for use in a low-clay translucent whiteware. *J Eur Ceram Soc* 2004;**24**: 2067–72.
19. Anstis GR, Chantikul T, Lawn BR, Marshall DB. A critical evaluation of indentation techniques for measuring fracture toughness: I, direct crack measurements. *J Am Ceram Soc* 1981;**64**:533–8.
20. Lide DR. *CRC handbook of chemistry and physics*. USA: CRC Press; 1992.
21. Andreola F, Barbieri L, Corradi A, Lancellotti I, Manfredini T. Utilisation of municipal incinerator grate slag for manufacturing porcelainized stoneware tiles manufacturing. *J Eur Ceram Soc* 2002;**22**:1457–62.
22. Ustundag CB, Tur YK, Capoglu A. Mechanical behaviour of a low-clay translucent whiteware. *J Eur Ceram Soc* 2006;**26**:169–77.
23. Taylor JR, Bull AC. *Ceramics glaze technology*. Oxford: Pergamon; 1986.
24. Krupkin YS, Rotenfel'd MM. Causes of crackle on porcelain ware. *Glass Ceram* 1971;**28**:382–3.
25. Kara A, Stevens R. Interactions between an ABS type leadless glaze and a biscuit fired bone china body during glost firing. Part II: investigation of interactions. *J Eur Ceram Soc* 2002;**22**:1103–12.